Auto-regressive model based input and parameter estimation for nonlinear finite element models

Juan Castiglione [a], Rodrigo Astroza [a,*], Saeed Eftekhar Azam [b], Daniel Linzell [b]

[a] Faculty of Engineering and Applied Sciences, Universidad de Los Andes, Chile
[b] Department of Civil Engineering, University of Nebraska-Lincoln, United States

ABSTRACT

A novel framework to accurately estimate nonlinear structural model parameters and unknown external inputs (i.e., loads) using sparse sensor networks is proposed and validated. The framework assumes a time-varying auto-regressive (TAR) model for unknown loads and develops a strategy to simultaneously estimate those loads and parameters of the nonlinear model using an unscented Kalman filter (UKF). First, it is confirmed that a Kalman filter (KF) allows to estimate TAR parameters for a measured, earthquake, acceleration time-history. The KF-based framework is then coupled to an UKF to jointly identify unmeasured inputs and nonlinear finite element (FE) model parameters. The proposed approach systematically assimilates different structural response quantities to estimate TAR and FE model parameters and, as a result, updates the FE model and unknown external excitation estimates. The framework is validated using simulated experiments on a realistic three-dimensional nonlinear steel frame subjected to unknown seismic ground motion. It is demonstrated that assuming relatively low order TAR model for the unknown input leads to precise reconstruction and unbiased estimation of nonlinear model parameters that are most sensitive to measured system response.

© 2020 Elsevier Ltd. All rights reserved.

1. Introduction

Estimating the remaining useful life of a structural system requires accurate identification of its current state of health and prediction of the effects of future demands. Distefano et al. [1] were among the first to posit the condition assessment of a structural system as a structural system identification problem. This requires identification of mechanistic, geometric, and/or damping properties of a computational model used to represent the physical structure. Given that variations in those properties can naturally affect a structure's dynamic response, vibration-based system identification methods have been extensively studied in the literature [2]. Vibration-based structural system identification can be approached as either (1) output-only or (2) input-output estimation problems. While the former category relies merely on measured structural response, the latter utilizes measurements of both excitation source and response of the structure to identify the structural system. Currently, application of output-only methods to large-scale structures is centered on using operational modal analysis (OMA) with inverse methods to calibrate a linear computational model of the structure using the OMA results. This framework is based on assuming that (1) structural response is linear and (2) random excitation is accurately represented using broad bandwidth power spectra. In many practical applications, such as for structures subjected to wind loads, vehicle

loads, and seismic ground motions, applied excitation violates the broadband assumption. In addition, many natural and man-made hazards, including earthquakes, blasts, and impact, induce nonlinear structural response. To account for non-stationary and non-broadband excitations and nonlinearities, response time histories can be directly incorporated into structural system identification, so that inputs, parameters, and potentially entire states of the system model are identified.

Identification of partially observed or hidden states of a system featuring measurement and modeling uncertainties is typically pursued within a Bayesian estimation framework. In a seminal work, the Kalman filter (KF) was developed to estimate the states of a linear system disturbed by white Gaussian measurement and process noises [3]. KF requires a priori knowledge of system inputs unless those inputs can be effectively assumed to be represented as broadband, stationary noise. To account for a general input type, Kitanidis developed a method for linear system state estimation in the presence of unknown or highly non-Gaussian system inputs [4]. Kitanidis proved that, although the filter was not globally optimum in the mean square error sense, it performs well when unknown inputs take extreme or unexpected values [4]. Hsieh developed a robust filter similar to that of Kitanidis for systems with unknown inputs and no direct feedthrough using a two-stage KF framework [5]. Gillijns and De Moor proposed a new filter, one that is globally optimal in the minimum-variance unbiased sense, for joint input and state (JIS) estimation for linear systems without direct feedthrough [6]. Gillijns and De Moor further extended their filter to systems that include a direct feedthrough term [7]. Lourens et al. utilized joint input-state estimation in structural systems [8]. Sedehi et al. developed a sequential Bayesian approach to estimate states and input of dynamic systems using output-only measurements [9]. Additionally, augmented Kalman filter (AKF) and dual Kalman filter (DKF) have been also developed to address structural input-state estimation problems [10,11]. Those methods were validated using laboratory experiments as well as experiments on large scale, in-service structural systems [12–14].

Linear and nonlinear state-space model parameter identification is typically conducted by defining a fictitious process equation for the unknown parameters and augmenting those parameters into the state vector. Even if original system behavior is linear, state-parameter estimation necessitates utilization of a nonlinear filtering technique. Extended Kalman filters (EKFs), which are based on linearization of state-space equations by truncating a Taylor series expansion of the nonlinear terms at each time step and using KF equations, have become the standard for weakly nonlinear systems disturbed by white Gaussian noise [15]. In many cases, linearization adopted by the EKF may be inaccurate and/or accurate calculation of the Jacobian not feasible. To account for these issues, Julier et al. proposed the unscented Kalman filter (UKF), where evolution of statistics representing the state of the system is performed using a deterministic sampling scheme [16]. The basic premise behind UKF is that sometimes it is more suitable to approximate the predictions of statistics of a state vector numerically, than analytically approximating its nonlinear evolution equation. Most existing work deals with joint state and parameter estimation of structural system phenomenological models and includes: linear and nonlinear shear building models [17–19]; linear trusses [20,21]; and nonlinear hysteretic models [22,23]. A small subset of published literature addresses state-parameter or parameter estimation of high-fidelity computational models of structural systems [24–27]. Astroza et al. developed a UKF-based parameter identification scheme for nonlinear finite element (FE) models [26] and showed that, for cases involving distributed plasticity within the system, smoothing yields a more accurate estimation of system parameters.

In the absence of input information, structural system identification becomes particularly challenging. To deal with this problem in a recursive Bayesian framework, Yang et al. proposed an adaptive EKF for structural damage identification in the presence of unknown inputs [28]. Lei et al. developed a framework for identification multi-story shear building response under unknown earthquake excitation using a substructuring method, an EKF, and partial output measurements, and validated it using numerical simulations and laboratory experiments [29]. Naets et al. developed an online, coupled, structural dynamics state/input/parameter estimation framework based on parametric model order reduction and EKF [30]. Several filtering and smoothing algorithms based on extension of JIS to nonlinear systems were recently developed [18,31,32]. Recursive Bayesian methods of input-state-parameter estimation research currently encompasses methods that extend EKF [28,33], UKF [34,35], and particle filters [19,36] to account for unknown inputs. Batch and sequential Bayesian methods have also been developed to address unknown input [37,38]. In similar fashion to published state-parameter estimation research, only a small fraction of existing literature deals with system identification using high fidelity, nonlinear structural system models in the presence of unknown inputs. Astroza et al. studied this problem by assessing the effects of input uncertainty on nonlinear FE model updating effectiveness for structural systems subjected to unmeasured seismic excitations [39].

In this paper, a novel framework is proposed for updating of high-fidelity nonlinear structural FE models subjected to unknown seismic excitations. Nonlinear model updating is divided into two parts: input estimation and parameter identification. While auto-regressive moving average (ARMA) models have been utilized to represent seismic excitations in the literature [40], the current study models input using a time-varying auto-regressive (TAR) model [41]. In addition, a random walk is implemented for time evolution of FE model parameters. An UKF is employed to jointly estimate TAR load and FE model parameters. Extensive simulated experiments demonstrate the precision and robustness of the developed framework.

The remainder of this paper is organized as follows. In Section 2 a detailed study is presented for TAR models utilized for replicating seismic ground motions and the proposed KF method for identification of its parameters. In Section 3 the detailed algorithm for input and parameter estimation of nonlinear FE models is developed. In Section 4 simulated experiments on a realistic steel frame are reported, and in Section 5 conclusions are drawn.

2. Time-varying auto-regressive (TAR) models for ground acceleration time histories

2.1. Problem formulation

The discrete-time equation of a TAR model of order p for the j-th component of a set of time histories, in this paper, ground accelerations, at time $t_{k+1} = (k+1)\Delta t$, in which $k = 0, 1, \ldots, N - 1$, Δt = time step, and N = number of samples, can be expressed as:

$$\ddot{s}_{k+1}^{(j)} = -\sum_{i=1}^{p} a_{k+1,i}^{(j)} \ddot{s}_{k+1-i}^{(j)} + e_{k+1}^{(j)} = \hat{\ddot{s}}_{k+1}^{(j)} + e_{k+1}^{(j)}, \tag{1}$$

where $\ddot{s}_{k+1}^{(j)} \in \mathbb{R}$ = j-th component of the measured ground acceleration at time step $(k + 1)$; $e_{k+1}^{(j)} \in \mathbb{R}$ = prediction error, which is assumed to be uncorrelated white Gaussian noise with zero-mean and standard deviation $\sigma_{k+1}^{(j)} \in \mathbb{R}$, i.e. $e_{k+1}^{(j)} \sim N\left(0, \sigma_{k+1}^{(j)}\right)$; $a_{k+1,i}^{(j)} \in \mathbb{R}$ = TAR model time-variant parameters; $p \in \mathbb{R}$ = TAR model order; and $\hat{\ddot{s}}_{k+1}^{(j)}$ = TAR model prediction of the j-th component of the ground acceleration at time step $(k + 1)$. Eq. (1) can be rewritten as:

$$\ddot{s}_{k+1}^{(j)} = \left(\mathbf{h}_k^{(j)}\right)^T \bar{\theta}_{k+1}^{inp\ (j)} + e_{k+1}^{(j)}, \tag{2}$$

where $\left(\mathbf{h}_k^{(j)}\right)^T \in \mathbb{R}^{1 \times p}$ = vector of ground accelerations at previous time steps and $\bar{\theta}_{k+1}^{inp\ (j)} \in \mathbb{R}^{p \times 1}$ = TAR model parameter vector at time t_{k+1}, i.e.:

$$\left(\mathbf{h}_k^{(j)}\right)^T = \begin{bmatrix} -\ddot{s}_k^{(j)} & -\ddot{s}_{k-1}^{(j)} & \cdots & -\ddot{s}_{k+1-p}^{(j)} \end{bmatrix}, \tag{3}$$

$$\bar{\theta}_{k+1}^{inp\ (j)} = \begin{bmatrix} a_{k+1,1}^{(j)} & a_{k+1,2}^{(j)} & \cdots & a_{k+1,p}^{(j)} \end{bmatrix}^T. \tag{4}$$

Utilizing Eqs. (3) and (4) allows to express Eq. (2) in vector form for n_s ground acceleration components at time step $(k + 1)$ as:

$$\ddot{\mathbf{s}}_{k+1} = diag\left(\mathbf{H}_k^T \mathbf{\Theta}_{k+1}^{inp}\right) + \tilde{\mathbf{e}}_{k+1} = \hat{\ddot{\mathbf{s}}}_{k+1} + \tilde{\mathbf{e}}_{k+1}, \tag{5}$$

where $\ddot{\mathbf{s}}_{k+1} \in \mathbb{R}^{n_s \times 1}$ = vector of ground accelerations measured at time step $(k + 1)$; $diag(\mathbf{A})$ represents the diagonal of matrix $\mathbf{A}$; $\tilde{\mathbf{e}}_{k+1} \in \mathbb{R}^{n_s \times 1}$ = uncorrelated white Gaussian noise prediction error vector having zero-mean and covariance matrix $\mathbf{R}_{k+1}^{inp} \in \mathbb{R}^{n_s \times n_s}$, i.e. $\tilde{\mathbf{e}}_{k+1} \sim N\left(\mathbf{0}, \mathbf{R}_{k+1}^{inp}\right)$; n_s = number of ground acceleration components; $\mathbf{H}_k^T \in \mathbb{R}^{n_s \times n_s}$ = matrix containing ground accelerations at previous time steps; and $\mathbf{\Theta}_{k+1}^{inp} \in \mathbb{R}^{p \times n_s}$ = matrix containing TAR model parameters. The ground acceleration vector and both matrices defining the TAR model prediction can be written as:

$$\ddot{\mathbf{s}}_{k+1} = \begin{bmatrix} \ddot{s}_{k+1}^{(1)} & \ddot{s}_{k+1}^{(2)} & \cdots & \ddot{s}_{k+1}^{(n_s)} \end{bmatrix}^T, \tag{6}$$

$$\mathbf{H}_k^T = \begin{bmatrix} -\ddot{s}_k^{(1)} & -\ddot{s}_{k-1}^{(1)} & \cdots & -\ddot{s}_{k+1-p}^{(1)} \\ -\ddot{s}_k^{(2)} & -\ddot{s}_{k-1}^{(2)} & \cdots & -\ddot{s}_{k+1-p}^{(2)} \\ \vdots & \vdots & \cdots & \vdots \\ -\ddot{s}_k^{(n_s)} & -\ddot{s}_{k-1}^{(n_s)} & \cdots & -\ddot{s}_{k+1-p}^{(n_s)} \end{bmatrix}, \tag{7}$$

$$\mathbf{\Theta}_{k+1}^{inp} = \begin{bmatrix} a_{k+1,1}^{(1)} & a_{k+1,1}^{(2)} & \cdots & a_{k+1,1}^{(n_s)} \\ a_{k+1,2}^{(1)} & a_{k+1,2}^{(2)} & \cdots & a_{k+1,2}^{(n_s)} \\ \vdots & \vdots & \cdots & \vdots \\ a_{k+1,p}^{(1)} & a_{k+1,p}^{(2)} & \cdots & a_{k+1,p}^{(n_s)} \end{bmatrix}. \tag{8}$$

Assuming that TAR model parameters are modeled as a random vector process according to the Bayesian estimation approach, its evolution can be described using a random walk process. This assumption together with Eq. (5) define the following linear state-space model:

$$\theta_{k+1}^{inp} = \theta_k^{inp} + \beta_k, \tag{9}$$

$$\ddot{\mathbf{s}}_{k+1} = diag\left(\mathbf{H}_k^T \mathbf{\Theta}_{k+1}^{inp}\right) + \tilde{\mathbf{e}}_{k+1},$$

where $\theta_{k+1}^{inp} = \left[\left(\bar{\theta}_{k+1}^{inp\,(1)}\right)^T, \left(\bar{\theta}_{k+1}^{inp\,(2)}\right)^T, ..., \left(\bar{\theta}_{k+1}^{inp\,(n_s)}\right)^T\right]^T \in \mathbb{R}^{p \cdot n_s \times 1}$ and $\beta_k \in \mathbb{R}^{p \cdot n_s \times 1}$ = process noise vector assumed to be stationary zero-mean white Gaussian noise with covariance matrix $\mathbf{Q}_k^{inp} \in \mathbb{R}^{p \cdot n_s \times p \cdot n_s}$, i.e., $\beta_k \sim N\left(\mathbf{0}, \mathbf{Q}_k^{inp}\right)$. This formulation permits using a Kalman filter (KF) to estimate the mean vector and covariance matrix of the TAR model parameters, θ^{inp}. When ground acceleration is directly measured, $\mathbf{H}_k^T$ is constructed using the measurements from preceding time steps. However, when a TAR parameter estimation problem is solved within an input-state estimation framework with ground acceleration not directly measured, matrix $\mathbf{H}_k^T$ is obtained from previous ground acceleration estimates. To ensure that the filter converges when estimating TAR model parameters at each time step, the KF correction step may include iterations until certain convergence criteria are satisfied. Fig. 1 depicts the pseudo code for the proposed algorithm that estimates the parameters of TAR models representing ground acceleration time histories.

It is noted that other parameterizations for earthquake ground motions could be considered instead of the TAR model. However, as shown in Section 2.2, a low order for TAR models is sufficient to properly reproduce seismic motions, which allows to have a reduced number of model parameters to be estimated. Other parametrizations (e.g., [42,43]) have great potential to be used with a batch estimation approach. In this study, a TAR model facilitates the estimation process since a recursive estimation approach is employed. On the other hand, no parametrization of the unknown input, e.g., assuming a random walk for the input sample, can also be considered (e.g., [39]). However, the parametrization of the input excitation allows reducing the computational cost involved in the estimation process.

2.2. Validation

The purpose of this section is to confirm that a well calibrated TAR model is able to properly represent an earthquake ground motion. Results are presented for the 1994 Northridge earthquake recorded at the Sylmar Country Hospital station. The 90° component of the earthquake motion is selected and, while results for only one earthquake ground motion are shown, consistent accuracy was obtained for a much larger set of strong motions but results of latter are not reported for the sake of brevity. Estimation of TAR model parameters ultimately aims to completely reconstruct an unknown ground

Initialize:	
$\hat{\theta}_{0|0}^{inp}$: Initial estimate of TAR model parameters	
$\hat{\mathbf{P}}_{0|0}^{inp}$: Initial covariance of TAR model parameters	
for $k = 0,1,...,N-1$	Loop over time steps
Prediction step:	
1. $\hat{\theta}_{k+1|k}^{inp} = \hat{\theta}_{k|k}^{inp}$	Prior estimate of TAR model parameters
2. $\hat{\mathbf{P}}_{k+1|k}^{inp} = \hat{\mathbf{P}}_{k|k}^{inp} + \mathbf{Q}_{k+1}^{inp}$	Prior covariance of TAR model parameters
Correction step is performed iteratively:	
3. $j = 0$; $\hat{\theta}_{k+1|k+1,j}^{inp} = \hat{\theta}_{k+1|k}^{inp}$; $\hat{\mathbf{P}}_{k+1|k+1,j}^{inp} = \hat{\mathbf{P}}_{k+1|k}^{inp}$ *while* $j < N_{iter}$	Initialize iterations
4. $\mathbf{K}_{k+1,j} = \hat{\mathbf{P}}_{k+1|k+1,j}^{inp} \mathbf{H}_k^T \left(\mathbf{H}_k \hat{\mathbf{P}}_{k+1|k+1,j}^{inp} \mathbf{H}_k^T + \mathbf{R}_{k+1}^{inp}\right)^{-1}$	Kalman gain
5. $\hat{\theta}_{k+1|k+1,j+1}^{inp} = \hat{\theta}_{k+1|k+1,j}^{inp} + \mathbf{K}_{k+1,j}\left[\ddot{\mathbf{s}}_{k+1} - diag\left(\mathbf{H}_k^T \hat{\theta}_{k+1}^{inp}\right)\right]$	Posterior estimate of TAR model parameters
6. $\hat{\mathbf{P}}_{k+1|k+1,j+1}^{inp} = \left(\mathbf{I} - \mathbf{K}_{k+1,j}\mathbf{H}_k\right)\hat{\mathbf{P}}_{k+1|k+1,j}^{inp}$	Posterior covariance of TAR model parameters
if $\left\|\hat{\theta}_{k+1|k+1,j+1}^{inp} - \hat{\theta}_{k+1|k+1,j}^{inp}\right\| \leq \varepsilon \left\|\hat{\theta}_{k+1|k+1,j}^{inp}\right\|$	Check for convergence
7. *break* *else*	

8. $j = j + 1$
 end if
 end while	

9. $\hat{\theta}_{k+1|k+1}^{inp} = \hat{\theta}_{k+1|k+1,j}^{inp}$	Final posterior estimate of TAR model parameters
10. $\hat{\mathbf{P}}_{k+1|k+1}^{inp} = \hat{\mathbf{P}}_{k+1|k+1,j}^{inp}$	Final posterior covariance of TAR model parameters
end for	

Fig. 1. TAR model calibration pseudo-code for representing earthquake ground motions.

acceleration time history for use in output-only nonlinear FE model updating. Since the objective is to simulate and estimate the input, it is assumed that the time history is measured using an accelerometer with the available measurement at time t_{k+1} being referred to as $\ddot{s}_{k+1}$. Note that this input is considered unknown or unmeasured in the following sections.

The initial estimate for the input ground acceleration is taken equal to $\hat{\ddot{s}}_{0|0} = [0.01] \, \text{m/s}^2 \in \mathbb{R}^{1 \times 1}$ and the initial estimate of the unknown TAR model parameters is $\hat{\theta}_{0|0}^{inp} = [0.1, ..., 0.1]^T \in \mathbb{R}^{p \times 1}$. The initial estimate of the covariance matrix is $\hat{P}_{0|0}^{inp} = 1.0 \times I_{p \times p}$, where $I_{l \times l} = l \times l$ identity matrix. The prediction error covariance matrix is taken as $R_{k+1}^{inp} = 0.1 \times I_{1 \times 1} \, (\text{m/s}^2)^2$ and the covariance matrix of the process noise vector is assumed to be $Q_{k+1}^{inp} = 1 \cdot 10^{-5} \times I_{p \times p}$. In this case, a maximum number of iterations, $N_{iter} = 3$, and a convergence criterion, $\varepsilon = 2\%$, are considered (see Fig. 1). Fig. 2 shows true input ground acceleration $\ddot{s}$ and estimated input ground acceleration $\hat{\ddot{s}}$ for various orders of the TAR model ($p = 5, 6,$ and 7). Note that, for this case study, $\Delta t = 0.02s$, $N = 600$, and $n_s = 1$. Excellent performance of the proposed algorithm is observed for the different order TAR models that were analyzed. It is also observed that, as the TAR model order increases, goodness-of-fit between true and estimated time histories, measured using relative root mean squared error (RRMSE), improves since the model accounts for additional information from previous time history steps. Recall that the RRMSE between two signals, sig^1 and sig^2, having N samples is defined as:

$$\text{RRMSE}\left(\text{sig}^1, \text{sig}^2\right) = \sqrt{\sum_{i=1}^{N}\left(\text{sig}_i^1 - \text{sig}_i^2\right)^2 / \sum_{i=1}^{N}\left(\text{sig}_i^1\right)^2} \times 100(\%).$$

(10)

3. Input and parameter estimation for nonlinear FE models

The dynamic response of a structural system can be obtained using a discrete-time equation of motion of a nonlinear FE model of the system. At discrete time t_{k+1}, this equation can be expressed as:

$$M\left(\theta^{fem}\right)\ddot{q}_{k+1}\left(\theta^{fem}\right) + C\left(\theta^{fem}\right)\dot{q}_{k+1}\left(\theta^{fem}\right) + r_{k+1}\left(q_{1:k+1}\left(\theta^{fem}\right)\right) = f_{k+1} + g_{k+1},$$

(11)

where $\theta^{fem} \in \mathbb{R}^{n_{fem} \times 1}$ = unknown model parameter vector of the FE model; n_{fem} = number of unknown FE model parameters; q, $\dot{q}$, $\ddot{q} \in \mathbb{R}^{n \times 1}$ = nodal displacement, velocity, and acceleration response vectors; n = number of degrees of freedom; $M \in \mathbb{R}^{n \times n}$ = mass matrix; $C \in \mathbb{R}^{n \times n}$ = damping matrix; $r(q(\theta)) \in \mathbb{R}^{n \times 1}$ = history-dependent internal resisting force vector; $f \in \mathbb{R}^{n \times 1}$ = vector of known external dynamic forces; $g \in \mathbb{R}^{n \times 1}$ = vector of unknown external dynamic forces; and the subscripts indicate the time step. This general formulation, including known and unknown excitations, is preferred because it allows to cover different cases that can be faced in practical applications, such as, partially measured excitations (e.g., problems involving soil-structure interaction, extended structures with sensors installed only at some supports, cases with malfunctioning sensors) and completely unmeasured excitations.

Considering the case of rigid-base seismic excitation, the external dynamic force vectors take the form $f_{k+1} = -ML_u\ddot{u}_{k+1}$ and $g_{k+1} = -ML_s\ddot{s}_{k+1}$, where $L_u \in \mathbb{R}^{n \times n_u}$ = known base excitation influence matrix; n_u = number of known acceleration base excitation components; $\ddot{u}_{k+1} \in \mathbb{R}^{n_u \times 1}$ = known input ground acceleration time histories; $L_s \in \mathbb{R}^{n \times n_s}$ = unknown base excitation influence matrix; n_s = number of unknown acceleration base excitation components; and $\ddot{s}_{k+1} \in \mathbb{R}^{n_s \times 1}$ = unknown input
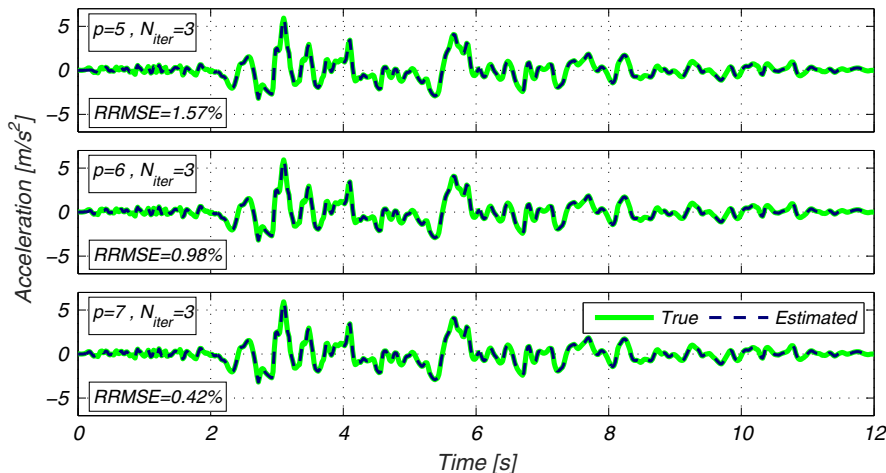

Fig. 2. True (actual) ground acceleration time history and estimated time histories based on TAR models of different orders.

ground acceleration time histories. As presented in Section 2, a TAR model can be used to represent the unknown input ground accelerations at each time step ($\ddot{\mathbf{s}}_{k+1}$). An augmented vector containing FE model parameters ($\boldsymbol{\theta}^{fem}$) and TAR model parameters ($\boldsymbol{\theta}^{inp}$) can then be defined as follows:

$$\boldsymbol{\theta} = \left[\left(\boldsymbol{\theta}^{fem} \right)^T \quad \left(\boldsymbol{\theta}^{inp} \right)^T \right]^T, \tag{12}$$

where $\boldsymbol{\theta} \in \mathbb{R}^{n_\theta \times 1}$ denotes the vector of unknown parameters to be estimated and $n_\theta = n_{fem} + n_s p$. The discrete-time equation of motion for the nonlinear FE model with unknown input parameterized using the TAR model can be written as:

$$\mathbf{M}\left(\boldsymbol{\theta}^{fem}\right)\ddot{\mathbf{q}}_{k+1}(\boldsymbol{\theta}) + \mathbf{C}\left(\boldsymbol{\theta}^{fem}\right)\dot{\mathbf{q}}_{k+1}(\boldsymbol{\theta}) + \mathbf{r}_{k+1}\left(\mathbf{q}_{1:k+1}(\boldsymbol{\theta})\right) = -\mathbf{M}\left(\boldsymbol{\theta}^{fem}\right)\left(\mathbf{L}_u\ddot{\mathbf{u}}_{k+1} + \mathbf{L}_s\ddot{\mathbf{s}}_{k+1}\left(\boldsymbol{\theta}^{inp}\right)\right). \tag{13}$$

According to Eq. (13), the response of the nonlinear FE model at time t_{k+1} can be expressed as a nonlinear function of FE model parameter vector ($\boldsymbol{\theta}^{fem}$), TAR model parameters ($\boldsymbol{\theta}^{inp}$), known input ground acceleration ($\ddot{\mathbf{u}}_{1:k+1}$), and initial conditions ($\mathbf{q}_0, \dot{\mathbf{q}}_0$) as

$$\hat{\mathbf{y}}_{k+1} = \mathbf{l}_{k+1}\left(\boldsymbol{\theta}^{fem}, \boldsymbol{\theta}^{inp}, \ddot{\mathbf{u}}_{1:k+1}, \mathbf{q}_0, \dot{\mathbf{q}}_0\right), \tag{14}$$

where $\hat{\mathbf{y}}_{k+1} \in \mathbb{R}^{n_y \times 1}$ = vector of predicted structural output response of the nonlinear FE model; $\mathbf{l}_{k+1}$ = nonlinear response function; $\mathbf{q}_0$ = initial displacement; and $\dot{\mathbf{q}}_0$ = initial velocity.

Actual response of a structure can be recorded using a heterogeneous array of sensors (e.g. accelerometers, strain-gauges, GPS and others) and can be related to the FE predicted response vector $\hat{\mathbf{y}}_{k+1}$ by:

$$\mathbf{y}_{k+1} = \hat{\mathbf{y}}_{k+1} + \mathbf{v}_{k+1}, \tag{15}$$

where $\mathbf{y}_{k+1} \in \mathbb{R}^{n_y \times 1}$ = vector of measured structural responses and $\mathbf{v}_{k+1} \in \mathbb{R}^{n_y \times 1}$ = simulation error vector assumed to be a stationary, zero-mean, white Gaussian noise process with covariance matrix $\mathbf{R}_{k+1} \in \mathbb{R}^{n_y \times n_y}$, i.e., $\mathbf{v}_{k+1} \sim N(\mathbf{0}, \mathbf{R}_{k+1})$.

The vector of measured responses from time t_1 to t_{k+1}, $\mathbf{y}_{1:k+1} = \left[\mathbf{y}_1^T, \mathbf{y}_2^T, ..., \mathbf{y}_{k+1}^T\right]^T$, can be expressed as a nonlinear function of the unknown parameter vector $\boldsymbol{\theta}$, $\ddot{\mathbf{u}}_{1:k+1}$, $\mathbf{q}_0$, $\dot{\mathbf{q}}_0$, and $\mathbf{v}_{1:k+1}$ (simulation error from t_1 to t_{k+1}, $\mathbf{v}_{1:k+1} = \left[\mathbf{v}_1^T, \mathbf{v}_2^T, ..., \mathbf{v}_{k+1}^T\right]^T \in \mathbb{R}^{n_y(k+1) \times 1}$) as:

$$\mathbf{y}_{1:k+1} = \mathbf{h}_{k+1}(\boldsymbol{\theta}, \ddot{\mathbf{u}}_{1:k+1}, \mathbf{q}_0, \dot{\mathbf{q}}_0) + \mathbf{v}_{1:k+1}, \tag{16}$$

where $\mathbf{h}_{k+1}(\cdot)$ is the nonlinear response function from t_1 to t_{k+1}.

Here, uncertainty in the unknown parameter vector ($\boldsymbol{\theta}$) is modeled as a random walk according to the Bayesian approach. The following nonlinear state-space model can then be formulated:

$$\boldsymbol{\theta}_{k+1} = \boldsymbol{\theta}_k + \mathbf{w}_k, \tag{17}$$

$$\mathbf{y}_{1:k+1} = \mathbf{h}_{k+1}(\boldsymbol{\theta}, \ddot{\mathbf{u}}_{1:k+1}, \mathbf{q}_0, \dot{\mathbf{q}}_0) + \mathbf{v}_{1:k+1},$$

where $\mathbf{w}_k \in \mathbb{R}^{n_\theta \times 1}$ = process noise assumed to be a stationary zero-mean white Gaussian noise with covariance matrix $\mathbf{Q}_k \in \mathbb{R}^{n_\theta \times n_\theta}$, i.e., $\mathbf{w}_k \sim N(\mathbf{0}, \mathbf{Q}_k)$. Note that it is assumed that different components of input ground acceleration time histories are uncorrelated, which is not expected in real earthquake records because of wave propagation path and surface geology effects. Although this assumption adds more flexibility to the time histories to be estimated, it does not affect the estimation process as shown latter in this paper. It is also assumed that, for Eq. (17), when updating the model and identifying the unknown input at time step $(k+1)$, the prior TAR model parameter estimates at that time step are equal to TAR model posterior parameters estimated at time step k.

An UKF is used to estimate unknown parameter vector $\boldsymbol{\theta}$, which contains unknown FE model parameters $\boldsymbol{\theta}^{fem}$ and unknown TAR model parameters $\boldsymbol{\theta}^{inp}$. At each time step, the first two statistical moments of $\boldsymbol{\theta}$, its mean vector $\hat{\boldsymbol{\theta}}$ and covariance matrix $\hat{\mathbf{P}}^{\theta\theta}$, are estimated using UKF given measured structure response ($\mathbf{y}$), measured input acceleration time history ($\ddot{\mathbf{u}}$), and unknown input acceleration time history ($\ddot{\mathbf{s}}$) that is reconstructed using estimated TAR model parameters. Fig. 3 depicts the pseudo-code that jointly estimates FE and TAR model parameters defining unknown ground acceleration time histories.

It is worth noting that alternative approaches in the literature have proposed using surrogate models for replacing computationally more expensive FE models (e.g., [44,45]). However, state-of-the-art mechanics-based nonlinear FE models which are able to capture the complex nonlinear behavior of civil structures, as those used in this paper, allows to better identify the damage in the structure, providing information about the presence, location, and extend of damage. In addition, current research on surrogate models have employed empirical-based nonlinear models, such as the Bouc-Wen model, and to our best knowledge, surrogate models for state-of-the-art modeling techniques for civil engineering structures have not yet been proposed in the literature.

Updating state-of-the-art nonlinear structural FE models involves significant computational cost and complex nonlinear FE models with high dimensional parameter spaces might make difficult to solve the inverse problem. Astroza et al. [46] recently proposed a simple two-step approach to deal with this problem in the case of structures subjected to measured seis-

Initialize:	
$\hat{\boldsymbol{\theta}}_{0\|0}$: Initial estimate of the unknown parameters	
$\hat{\mathbf{P}}_{0\|0}^{\boldsymbol{\theta\theta}}$: Initial covariance of the unknown parameters	
for $k = 0, 1, \ldots, N-1$	Loop over time steps
Prediction step:	
1. $\hat{\boldsymbol{\theta}}_{k+1\|k} = \hat{\boldsymbol{\theta}}_{k\|k}$	Prior estimate
2. $\hat{\mathbf{P}}_{k+1\|k}^{\boldsymbol{\theta\theta}} = \hat{\mathbf{P}}_{k\|k}^{\boldsymbol{\theta\theta}} + \mathbf{Q}_{k+1}$	Prior covariance
Correction step:	
3. $j = 0$; $\hat{\boldsymbol{\theta}}_{k+1\|k+1,j} = \hat{\boldsymbol{\theta}}_{k+1\|k}$; $\hat{\mathbf{P}}_{k+1\|k+1,j}^{\boldsymbol{\theta\theta}} = \hat{\mathbf{P}}_{k+1\|k}^{\boldsymbol{\theta\theta}}$	Initialize iterations
while $j < N_{iter}$	
4. $\vartheta_{k+1,j}^{(i)}$ $i = 1, \ldots, (2n_\theta + 1)$ based on $\hat{\boldsymbol{\theta}}_{k+1\|k+1,j}, \hat{\mathbf{P}}_{k+1\|k+1,j}^{\boldsymbol{\theta\theta}}$	Generate SPs
5. $\gamma_{1:k+1,j}^{(i)} = \mathbf{I}_{k+1}\left(\vartheta_{k+1,j}^{(i)}, \ddot{\mathbf{u}}_{1:k+1}\right)$	Output for each SP
6. $\hat{\mathbf{y}}_{1:k+1\|k,j} = \sum_{i=1}^{2n_\theta+1} W_m \gamma_{1:k+1,j}^{(i)}$	Predicted output
7. $\hat{\mathbf{P}}_{k+1\|k,j}^{\mathbf{yy}} = \sum_{i=1}^{2n_\theta+1} W_c^{(i)}\left[\gamma_{1:k+1,j}^{(i)} - \hat{\mathbf{y}}_{1:k+1\|k,j}\right]\left[\gamma_{1:k+1,j}^{(i)} - \hat{\mathbf{y}}_{1:k+1\|k,j}\right]^T + \mathbf{R}_{k+1}$	Estimated output covariance
8. $\hat{\mathbf{P}}_{k+1\|k,j}^{\boldsymbol{\theta}\mathbf{y}} = \sum_{i=1}^{2n_\theta+1} W_c^{(i)}\left[\vartheta_{k+1,j}^{(i)} - \hat{\boldsymbol{\theta}}_{k+1\|k,j}\right]\left[\gamma_{1:k+1,j}^{(i)} - \hat{\mathbf{y}}_{k+1\|k,j}\right]^T$	Estimated cross-covariance
9. $\mathbf{K}_{k+1,j} = \hat{\mathbf{P}}_{k+1\|k,j}^{\boldsymbol{\theta}\mathbf{y}}\left(\hat{\mathbf{P}}_{k+1\|k,j}^{\mathbf{yy}}\right)^{-1}$	Kalman gain
10. $\hat{\boldsymbol{\theta}}_{k+1\|k+1,j+1} = \hat{\boldsymbol{\theta}}_{k+1\|k+1,j} + \mathbf{K}_{k+1,j}(\mathbf{y}_{1:k+1} - \hat{\mathbf{y}}_{1:k+1\|k,j})$	Posterior estimate
11. $\hat{\mathbf{P}}_{k+1\|k+1,j+1}^{\boldsymbol{\theta\theta}} = \hat{\mathbf{P}}_{k+1\|k+1,j}^{\boldsymbol{\theta\theta}} - \mathbf{K}_{k+1,j}\hat{\mathbf{P}}_{k+1\|k,j}^{\mathbf{yy}}\mathbf{K}_{k+1,j}^T$	Posterior covariance
if $\left\|\hat{\boldsymbol{\theta}}_{k+1\|k+1,j+1}^{inp} - \hat{\boldsymbol{\theta}}_{k+1\|k+1,j}^{inp}\right\| \le \varepsilon\left\|\hat{\boldsymbol{\theta}}_{k+1\|k+1,j}^{inp}\right\|$	Check convergence of TAR model parameters
break	
else	
12. $j = j+1$	
end if	
end while	
13. $\hat{\boldsymbol{\theta}}_{k+1\|k+1} = \hat{\boldsymbol{\theta}}_{k+1\|k+1,j}$	Final posterior estimate
14. $\hat{\mathbf{P}}_{k+1\|k+1} = \hat{\mathbf{P}}_{k+1\|k+1,j}$	Final covariance estimate
end for	

Fig. 3. Nonlinear FE model updating pseudo-code incorporating unknown input using TAR model.

mic excitation, consisting on a one-at-a-time sensitivity analysis and a batch-recursive estimation approach. However, it is out of the scope of this paper to investigate and extend that formulation to the case of models with unknown input excitations.

4. Simulated experiments

4.1. Structural system and input excitation

To validate the proposed methodology, a three-dimensional, 4-story, steel framed, building was studied (Fig. 4). This structure was designed according to the 2012 International Building Code [47]. The building is assumed to be located in downtown Seattle (class D soil), so its short-period spectral acceleration and one-second spectral acceleration are S_{MS} = 1.37 g and S_{M1} = 0.53 g, respectively. The columns are 3.5 m in height with corner and interior columns being W14×61 and W14×90, respectively. Longitudinal beams (global X) have a length of 7.0 m and are W21×62 for floors 2 and 3 and W21×55 for floor 4 and the roof. Beams in the transverse direction (Z) are 8.0 m long and are W18×40 for levels 2 and 3 and W18×35 for levels 4 and roof. All the columns are made of A992 Grade 50 steel while the beams are made of A36 steel.
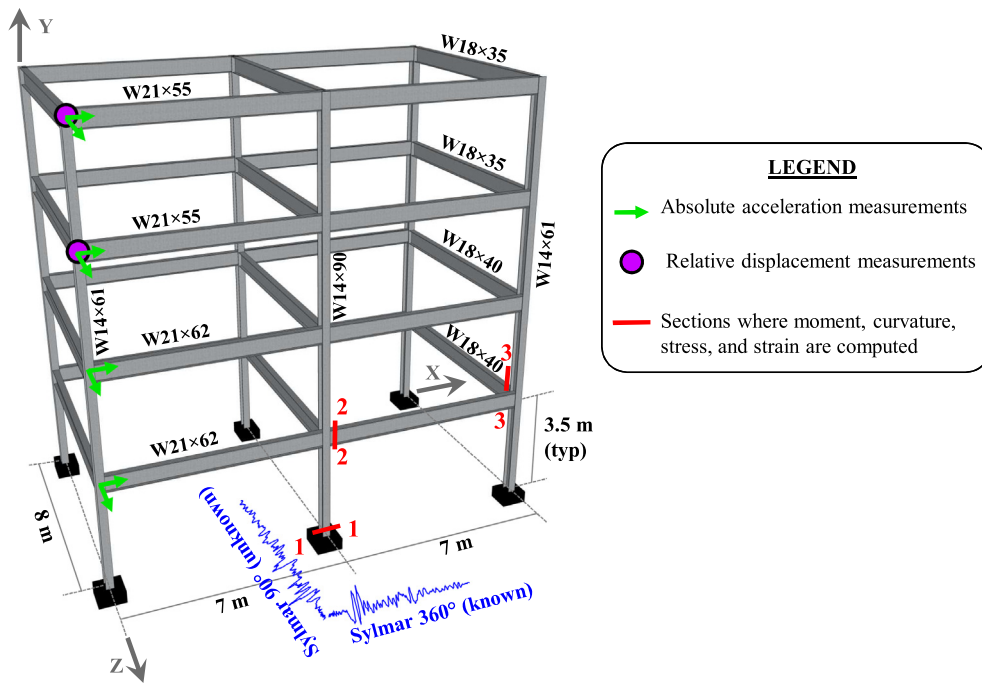
Fig. 4. 3-D steel frame structure.

Ground accelerations from the 1994 Northridge earthquake recorded at the Sylmar Country Hospital station were selected as base excitations. Fig. 5 depicts the two horizontal components of the earthquake, which were recorded at a sampling frequency of 50 Hz (i.e., $\Delta t = 0.02$), had a total number of samples $N = 600$, and reached peak ground accelerations of 0.84 g for the 360° component and 0.60 g for the 90° component.

4.2. Finite element model

The building was modeled in OpenSees [48] using mechanics-based, nonlinear, fiber-section, beam-column elements utilizing a force-based formulation [49]. For each beam and column member, a single force-based element was used, seven integration points (IPs) were considered along its length, and Gauss-Lobatto quadrature was employed. Note that the number of IPs was chosen such that the tributary length of the extreme IPs equaled the anticipated size of plastic hinges. Uniaxial
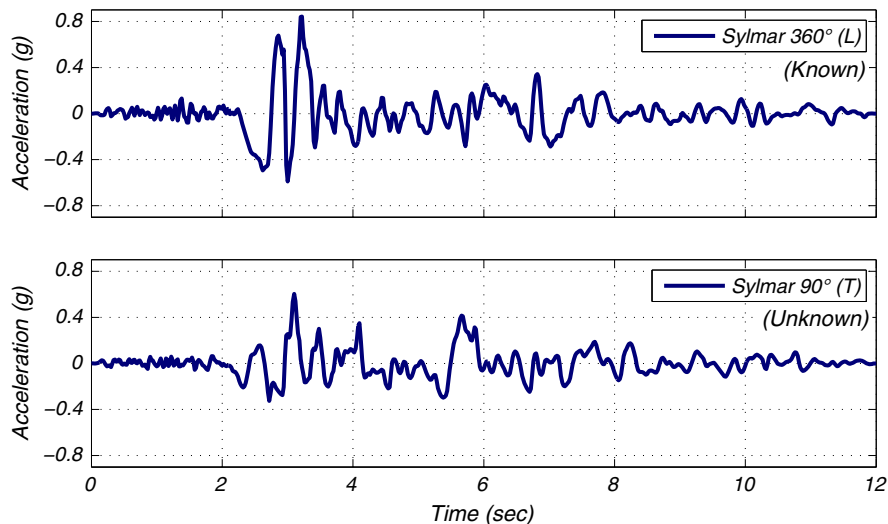

Fig. 5. Input base excitation time histories.

stress-strain behavior of the steel fibers was assumed to be governed by the modified, nonlinear, Giuffré-Menegotto-Pinto material constitutive law [50]. This material model characterizes cyclic inelastic behavior of the steel fibers through eight time-invariant parameters. For this study, these parameters were subdivided into primary and secondary groups based on their influence on global structural response measurements taken from real-world tests. The three primary parameters included the elastic modulus (E), initial yield strength (f), and strain-hardening ratio (b), while the secondary parameters were those that control curvature of hysteresis loops and isotropic hardening [51]. Primary parameters were considered as unknowns during the estimation phase with secondary parameters remaining fixed. Rayleigh damping was also included in the model considering a critical damping ratio of $\xi = 2\%$ for the building's first two initial longitudinal modes. Fig. 6 depicts assigned nodal masses, distributed beam dead and live loads taken from the 2012 International Building Code, and FE model geometry.

4.3. Response simulation

Response of the structural system was simulated considering base excitations from both horizontal ground motion components recorded at the Sylmar station (Figure 5) during the Northridge 1994 earthquake. As stated in the previous section, designated primary parameters were eventually considered as unknowns and can be depicted using the following vector:

$$\boldsymbol{\theta}^{fem} = [\; E_{col} \quad f_{col} \quad b_{col} \quad E_{beam} \quad f_{beam} \quad b_{beam} \;]^T \in \mathbb{R}^{6 \times 1} \tag{18}$$

To simulate structural response, the following primary parameter values, referred to as true parameters, were selected:

$$\boldsymbol{\theta}^{fem,true} = \left[\; E_{col}^{true} \quad f_{col}^{true} \quad b_{col}^{true} \quad E_{beam}^{true} \quad f_{beam}^{true} \quad b_{beam}^{true} \;\right]^T, \tag{19.a}$$

$$\boldsymbol{\theta}^{fem,tue} = [\; 200\,\text{GPa} \quad 345\,\text{MPa} \quad 0.04 \quad 200\,\text{GPa} \quad 250\,\text{MPa} \quad 0.03 \;]^T. \tag{19.b}$$

Simulated building response using these true parameters, referred to as the true response, were determined using the FE model described in Section 4.1 subjected to earthquake ground motions shown in Fig. 5. True responses were subsequently contaminated using zero mean white Gaussian noise to account for measurement uncertainty.

Note that one set of material model parameters for each type of steel (A992 for columns and A36 for beams) was considered. This is a valid assumption if all cross-sections of a steel grade were fabricated during the same manufacturing process.
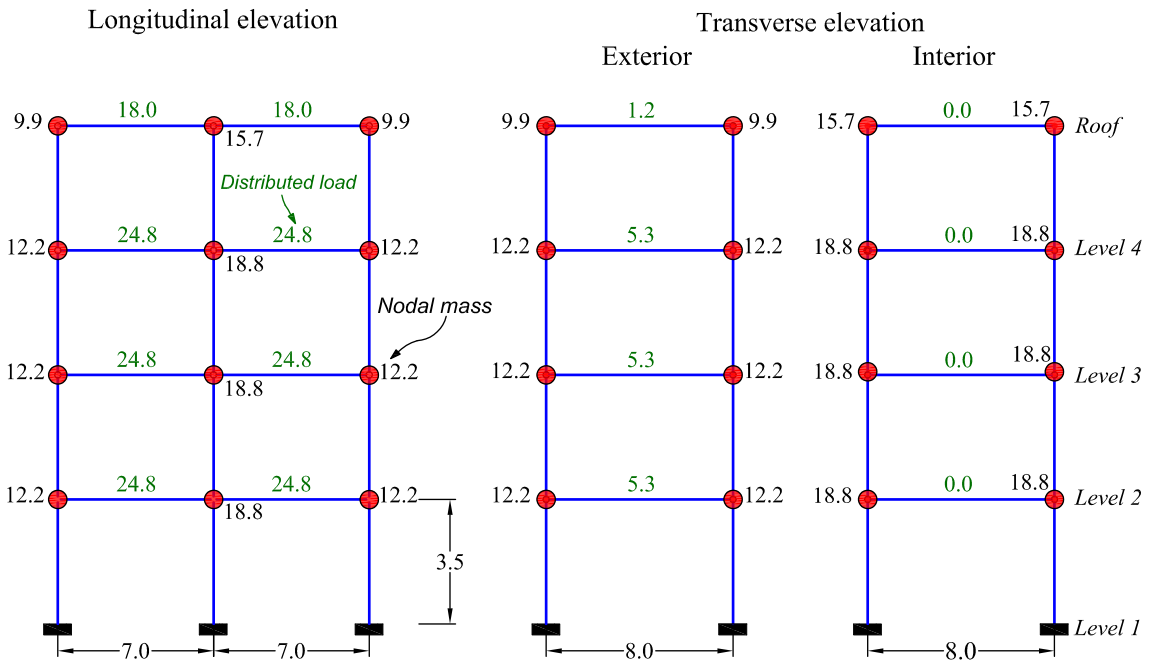

Fig. 6. 3-D steel frame finite element model.

4.4. Sensitivity study

Quantifying sensitivity of various measurement types and locations to variations in model parameters is crucial for correctly developing a sensor network and for updating the companion numerical model. To circumvent problems associated with unidentifiability of model parameters, various methods for quantifying and visualizing sensitivity have been developed. Tornado diagrams, which sort parameters based on the sensitivity of measured response to a designated variation in their value, were selected for the current study [52]. This is a simple, single-variate, sensitivity analysis in which each unknown model parameter is individually perturbed around its true value by ±5% with other parameters being fixed. Measured responses for each perturbed model subjected to Sylmar ground motions were computed and compared to those obtained from the true model using RRMSE. A large RRMSE implied that the response was sensitive to the corresponding model parameter and depicted using longer swings in the tornado diagram.

It was assumed that absolute accelerations in both horizontal directions could be measured at every level and relative displacements measured at Level 4 and the roof (see Fig. 4). Fig. 7 shows the tornado diagrams associated with roof absolute longitudinal (X axis in Fig. 4) acceleration and relative longitudinal displacement, which are both included in the instrumentation plans (see Fig. 4) used for FE model updating later. Both roof absolute acceleration and the relative displacement are more sensitive to the modulus of elasticity of the beam (E_{beam}) and column (E_{col}) fibers and less sensitive to material hardening ratios (b_{beam} and b_{col}). Absolute acceleration was observed to be slightly less sensitive to parameters governing the structure post-yield nonlinear behavior than relative displacement. Sensitivity analysis results for other observed responses follow similar trends to those presented here.

4.5. Parameter and input estimations

It was assumed that exact values for the six primary material model parameters in Eq. (19) and the transverse input excitation (i.e., 90° component of the Sylmar record) were unknown, i.e., $n_{fem} = 6$, $n_s = 1$, and $n_\theta = 6 + 1 \cdot p$. Note that considering one unknown input earthquake component mimics a real situation with a malfunctioning sensor at the base of a building. Eighteen different estimation cases were analyzed considering different orders of the TAR model and with and without iterations in the UKF correction step (see Fig. 3). These cases were chosen to study and evaluate convergence and performance of the proposed algorithm for estimating FE model parameters and unknown input excitation and to analyze computational costs. Cases ID1 to ID9 assumed that eight absolute acceleration responses were recorded (i.e., both horizontal components are each floor). Cases ID10 to ID18 assumed that four relative displacement responses (at levels four and the roof) were measured in addition to the eight accelerations. Measurement locations are shown in Fig. 4. As stated earlier, response data used to estimate the unknown material model parameters and input excitations were simulated using true responses presented in Section 4.3 corrupted by zero-mean white Gaussian noise having root-mean-square amplitudes of 0.5% g and 2 mm for the accelerations and displacements, respectively. Note that accelerometers record absolute accelerations, therefore this type of measurement is considered (it is not realistic to consider relative acceleration as measurement). Then, during model updat-
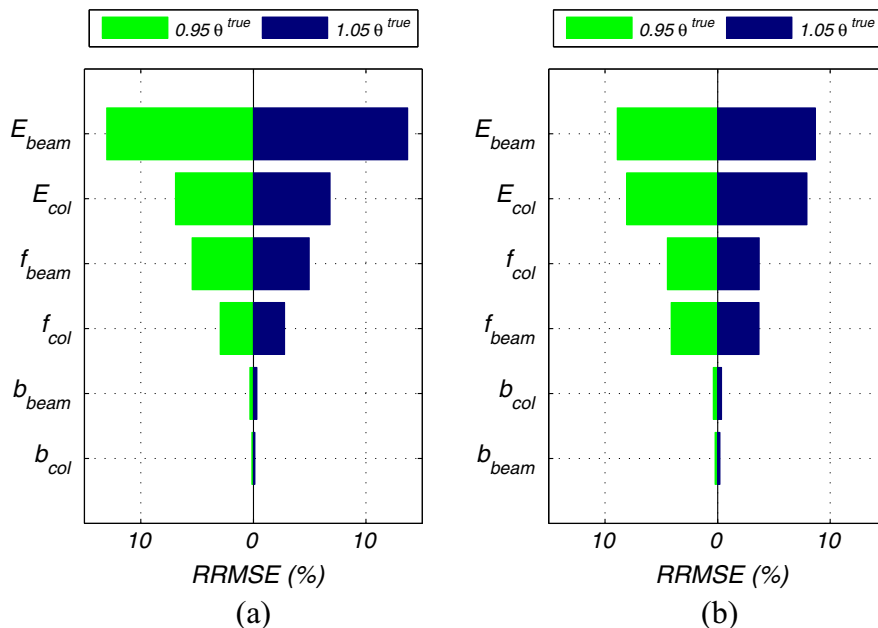

Fig. 7. RRMSE tornado diagrams for: (a) roof absolute longitudinal acceleration; and (b) roof relative longitudinal displacement.

ing, absolute acceleration responses are computed by adding the relative responses obtained from the model (see Eq. (13)) and the estimated input excitation.

The initial unknown input excitation estimate was taken equal to $\hat{\mathbf{s}}_{0|0} = [0.01]\,\text{m/s}^2 \in \mathbb{R}^{1\times 1}$ and the initial TAR model unknown parameter estimate was $\hat{\boldsymbol{\theta}}_{0|0}^{inp} = [0.1, ..., 0.1]^T \in \mathbb{R}^{p\times 1}$. The initial FE model parameter estimate was assumed as $\hat{\boldsymbol{\theta}}_{0|0}^{fem} = \left[\begin{array}{cccccc} 1.4 \cdot E_{col}^{true} & 0.7 \cdot f_{col}^{true} & 0.8 \cdot b_{col}^{true} & 1.5 \cdot E_{beam}^{true} & 0.8 \cdot f_{beam}^{true} & 1.3 \cdot b_{beam}^{true} \end{array}\right]^T \in \mathbb{R}^{6\times 1}$. The initial covariance matrix $\hat{\mathbf{P}}_{0|0}^{\theta\theta}$ was assumed to be diagonal, i.e., initial unknown input excitation parameters and FE model were statistically uncorrelated. Diagonal terms are chosen as $\left(\hat{\mathbf{P}}_{0|0}^{\theta\theta}\right)_{i,i} = \left(0.05 \times \hat{\boldsymbol{\theta}}_{0|0}^{fem}\right)^2$ for $i = 1, ..., n_{fem}$, which corresponded to FE model parameter covariance, and $\left(\hat{\mathbf{P}}_{0|0}^{\theta\theta}\right)_{i,i} = \left(1.00 \times \hat{\boldsymbol{\theta}}_{0|0}^{inp}\right)^2$ for $i = n_{fem} + 1, ..., n_{fem} + p \cdot n_s$, which corresponded to TAR model parameter covariance. Corresponding acceleration and displacement response on the diagonal for $\mathbf{R}$ were $9 \cdot 10^{-4}\,(\text{m/s}^2)^2$ and $2.25\,\text{mm}^2$, respectively. The process noise was assumed time-invariant and with diagonal entries equal to $\left(1 \cdot 10^{-5} \times \hat{\boldsymbol{\theta}}_{0|0}^{inp}\right)^2$ for the TAR model parameters and $\left(1 \cdot 10^{-6} \times \hat{\boldsymbol{\theta}}_{0|0}^{fem}\right)^2$ for the FE model parameters.

Table 1 lists FE model parameter estimation results corresponding to eighteen case studies that considered different outputs (i.e., acceleration and acceleration + displacement), TAR model orders $p = \{4, 6, 10\}$ and number of iterations $N_{iter} = \{0, 2, 3\}$. Precise estimates are observed for the elastic modulus and yield stress for all cases, with relative errors lower than 3%. However, strain hardening ratio estimates featured significant bias and were attributed to lower sensitivity of measured response to these parameters as discussed and shown in Section 4.4. Estimates did not significantly improve when displacement responses were considered in addition to accelerations. Note that parameter estimates with relative errors less than or equal to 5% are shaded in grey in Table 1.

Table 2 shows the RRMSEs between true and estimated input excitations, with estimated values developed using TAR model parameter estimates. Input estimates slightly improved when displacement responses were considered in addition to accelerations. The effects of adding iterations and increasing TAR model order were negligible in both FE model and unknown input estimates.

Two representative case studies are discussed in more detail. The first corresponded to case ID1, which considered a TAR model of order $p = 4$ without iterations. The second case is ID18, which considered $p = 10$ and three iterations. Fig. 8 shows time histories based on FE models using estimated parameters from each of these cases. Both cases showed precise performance of the proposed algorithm for estimation of the primary FE model parameters in the presence of unknown seismic inputs. Estimates for the beam and column fiber moduli (E_{col} and E_{beam}) and yield stresses (f_{col} and f_{beam}) converged to their true values while hardening ratio parameters (b_{col} and b_{beam}) did not converge. The elastic moduli of beams and columns converged in the first 0.5 s of the analyses, prior to the structure entering the nonlinear response regime. When the nonlinear
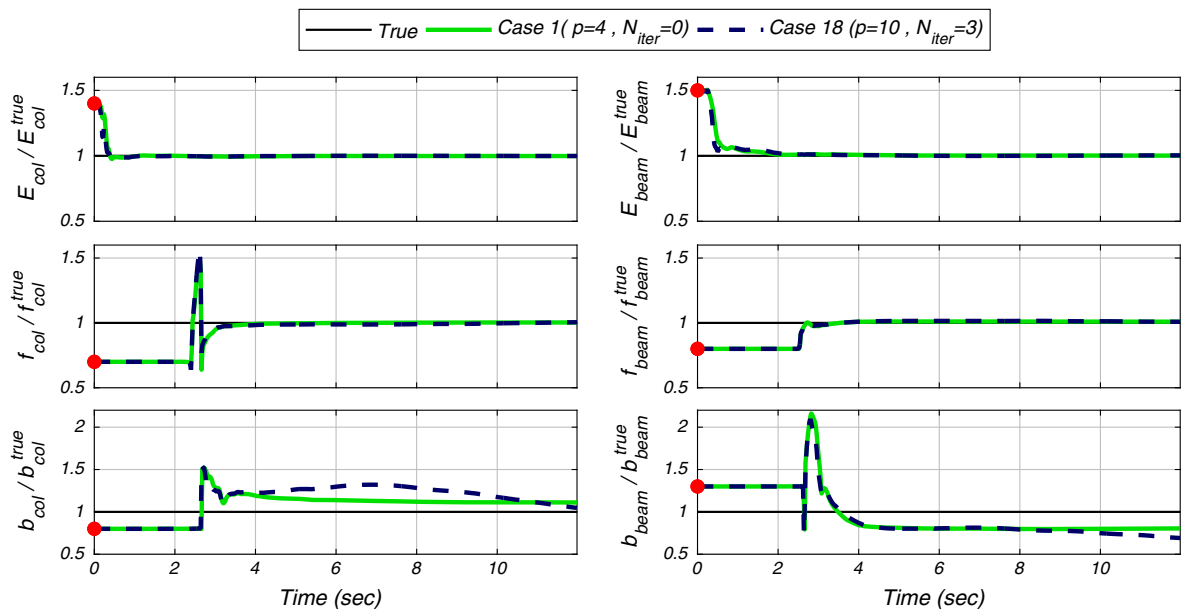
Table 1
Parameter estimation results.

Response measurement	Case ID	p	N_{iter}	Model parameter					
				$\dfrac{E_{col}}{E_{col}^{true}}$	$\dfrac{f_{col}}{f_{col}^{true}}$	$\dfrac{b_{col}}{b_{col}^{true}}$	$\dfrac{E_{beam}}{E_{beam}^{true}}$	$\dfrac{f_{beam}}{f_{beam}^{true}}$	$\dfrac{b_{beam}}{b_{beam}^{true}}$
Acceleration	1	4	NO	1.00	1.00	1.11	1.00	1.01	0.80
	2	4	2	1.00	1.00	1.07	1.00	1.01	0.84
	3	4	3	1.00	1.00	1.07	1.00	1.01	0.83
	4	6	NO	1.00	1.00	1.09	1.00	1.01	0.80
	5	6	2	1.00	1.00	1.07	1.00	1.01	0.84
	6	6	3	1.00	1.00	1.07	1.00	1.01	0.83
	7	10	NO	1.00	1.00	1.21	1.00	1.01	0.76
	8	10	2	1.00	1.00	1.16	1.00	1.01	0.79
	9	10	3	1.00	1.00	1.12	1.00	1.01	0.82
Acceleration + Displacement	10	4	NO	1.00	1.00	1.25	1.00	1.02	0.68
	11	4	2	1.00	1.01	0.82	1.01	1.00	0.69
	12	4	3	1.00	1.01	0.82	1.01	1.00	0.73
	13	6	NO	1.00	1.01	0.97	1.00	1.01	0.72
	14	6	2	1.00	1.02	0.74	1.01	1.00	0.65
	15	6	3	1.00	1.01	0.92	1.01	1.01	0.69
	16	10	NO	1.00	0.98	1.52	1.00	1.03	0.67
	17	10	2	1.00	1.00	1.08	1.00	1.01	0.69
	18	10	3	1.00	1.01	1.05	1.00	1.01	0.69

Table 2
RRMSEs for true and estimated earthquake input motions.

Response measurement	Case ID	p	N_{iter}	$RRMSE_{input}$ (%)	$RRMSE_{input}$ (%) – Filtered
Acceleration	1	4	NO	11.1	4.1
	2	4	2	12.3	4.1
	3	4	3	11.9	4.1
	4	6	NO	10.7	3.9
	5	6	2	11.6	4.0
	6	6	3	11.7	4.1
	7	10	NO	11.7	4.3
	8	10	2	11.7	4.1
	9	10	3	11.6	4.0
Acceleration + Displacement	10	4	NO	10.2	4.1
	11	4	2	10.1	4.1
	12	4	3	9.2	4.2
	13	6	NO	8.4	3.9
	14	6	2	11.7	4.2
	15	6	3	10.1	4.1
	16	10	NO	11.2	4.2
	17	10	2	9.6	4.0
	18	10	3	10.7	4.0

Fig. 8. Model parameter estimation time histories for Case ID1 and ID18.

response of the structure begins at about 2.5 s, the yield stresses and hardening ratios start to update and the former quickly converge to their true values. Although the case presented considers six unknown model parameters, other cases including eighteen model parameters (one set of material model parameters for each element cross-section) were also analyzed and results consistent to those reported here were obtained.

Fig. 9 compares true and estimated input motions for case studies ID1 and ID18. RRMSEs are practically the same for both cases, with a difference lower than 0.5%. Since a low-frequency component is observed in the estimated inputs, a high-pass Butterworth filter of order 7 and cut-off frequency at 0.15 Hz is applied. RRMSEs between filtered estimated and true input excitations are also shown in Table 2. It is observed that errors are all lower than 5.0%, indicating excellent estimation of unknown input excitation using the proposed framework, even when using a lower order TAR model (p = 4) with no iterations (N_{iter} = 0). Observed low-frequency as force estimation drift has been previously reported in the literature [10,39]. Formal observability and identifiability studies for nonlinear structural systems subjected to unknown inputs are rare, and the subject is an open research area. In this regard, Maes et al. developed a geometric algorithm based on Lie algebra to investigate the theoretical observability of nonlinear systems with partially measured inputs and outputs [53]. Their algorithm
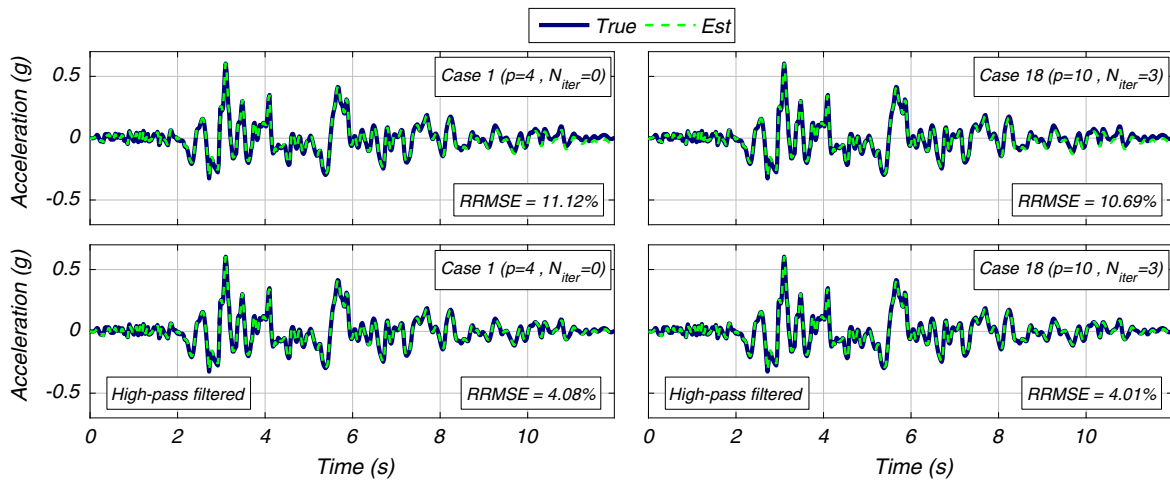
Fig. 9. True and estimated input earthquake motions for Case ID1 and ID18.

assumes that the measurements are continuous over time; therefore, it cannot be adopted for systems featuring discrete state space equations.

4.6. Errors between measured and unobserved responses

RRMSEs corresponding to measured response quantities used in the estimation process for the eighteen cases described in Section 4.5 are reported in Table 3. RRMSEs between true responses (without noise) and those obtained from final FE model parameter and input estimates (without high-pass filtering) are reported. Practically all acceleration responses exhibit an error lower than 10%, while measured displacements show errors between 10 and 15%, confirming a very good agreement between true and estimated responses. Fig. 10 compares true and estimated acceleration time histories in the building's transverse direction (i.e., direction of unknown input) for ID1 and ID18 and excellent agreement is observed.

Since prediction of unobserved (unmeasured) structural response is crucial for optimal and effective structural health monitoring and subsequent damage identification, RRMSEs for local, unobserved response quantities are also investigated. Moment, curvature, strain, and stress are analyzed with critical column and beam sections selected and responses from the true FE model subjected to the true excitation compared to those obtained from final estimates of FE model parameters and estimated unfiltered input. Table 4 shows RRMSEs for the eighteen case studies, with bending moment and curvature at the bottom of a column (Section 1-1 in Fig. 4) and at the end of longitudinal beam (Section 2-2) and stress and strain at the same column section and at the end of a transverse beam (Section 3-3) being studied. For most responses, very low RRMSEs are

Table 3
RRMSEs of measured responses.

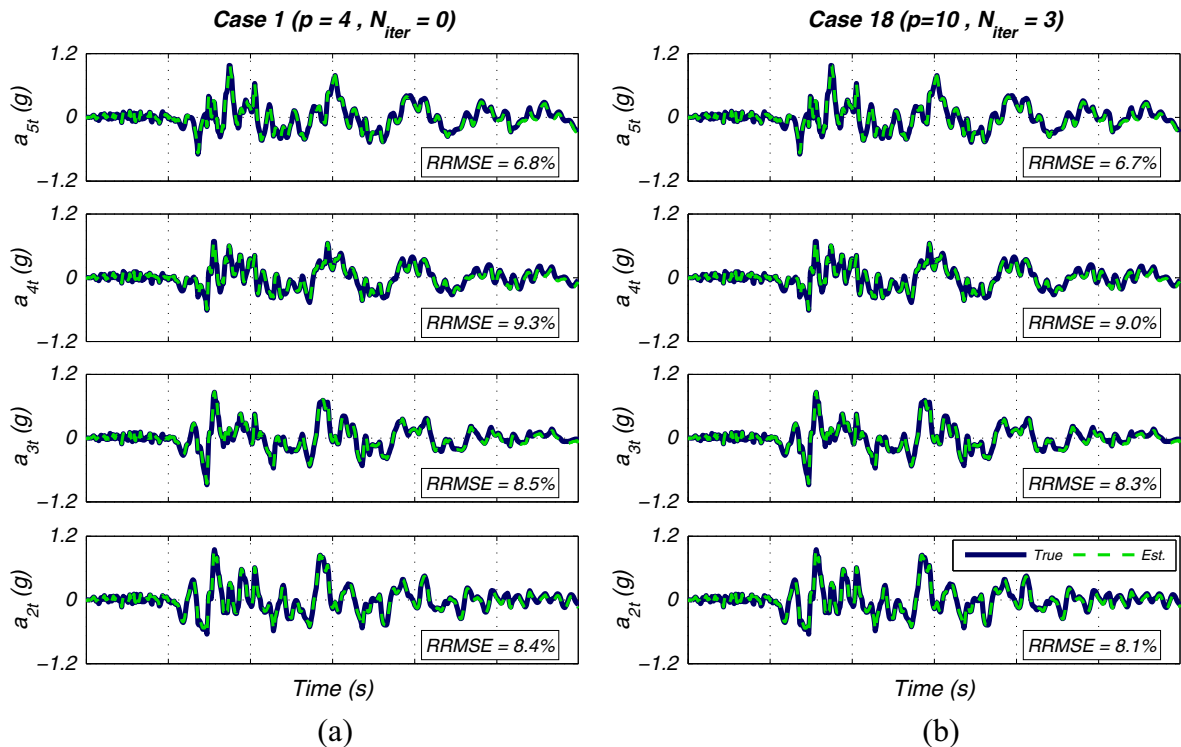| Response measurement	Case ID	p	N_{iter}	RRMSE (%) – Measured response					
				$\mathbf{a}_{2t}$	$\mathbf{a}_{3t}$	$\mathbf{a}_{4t}$	$\mathbf{a}_{5t}$	$\mathbf{d}_{4t}$	$\mathbf{d}_{5t}$
Acceleration	1	4	NO	8.4	8.5	9.3	6.8	–	–
	2	4	2	9.2	9.4	10.1	7.5	–	–
	3	4	3	8.9	9.1	9.8	7.3	–	–
	4	6	NO	8.1	8.2	8.9	6.6	–	–
	5	6	2	8.6	8.8	9.5	7.0	–	–
	6	6	3	8.8	8.9	9.7	7.2	–	–
	7	10	NO	9.1	9.1	10.1	7.4	–	–
	8	10	2	8.9	9.0	9.8	7.2	–	–
	9	10	3	8.7	8.9	9.6	7.1	–	–
Acceleration + Displacement	10	4	NO	7.9	7.9	8.8	6.5	13.1	14.0
	11	4	2	7.7	7.9	8.5	6.4	13.9	13.3
	12	4	3	7.2	7.3	7.8	5.9	11.7	11.2
	13	6	NO	6.6	6.7	7.2	5.4	11.0	10.6
	14	6	2	8.8	9.1	9.7	7.3	15.9	15.2
	15	6	3	7.8	7.9	8.6	6.4	12.9	12.3
	16	10	NO	8.8	8.7	9.8	7.2	14.3	13.7
	17	10	2	7.4	7.5	8.2	6.0	12.4	11.9
	18	10	3	8.1	8.3	9.0	6.7	13.6	13.1

Fig. 10. Comparison between true and estimated responses for (a) Case 1 and (b) Case ID18.

Table 4
RRMSEs of unmeasured responses.

Response measurement	Case ID	p	N_{iter}	*RRMSE* (%) – Unmeasured response							
				M_z^{1-1}	κ_z^{1-1}	M_z^{2-2}	κ_z^{2-2}	σ_{1-1}	ε_{1-1}	σ_{3-3}	ε_{3-3}
Acceleration	1	4	NO	1.4	6.9	1.9	7.0	1.4	8.0	1.4	6.0
	2	4	2	1.0	4.8	1.6	5.9	1.0	5.3	1.1	5.5
	3	4	3	1.0	4.5	1.6	6.0	1.1	5.2	1.2	5.4
	4	6	NO	1.2	5.7	2.0	7.0	1.4	6.7	1.5	5.8
	5	6	2	1.0	4.7	1.6	6.0	1.1	5.4	1.2	5.5
	6	6	3	1.0	4.8	1.7	6.2	1.1	5.6	1.2	5.5
	7	10	NO	1.7	11.6	2.5	8.4	2.4	13.3	1.9	5.9
	8	10	2	1.5	9.1	2.1	7.8	1.9	10.5	1.7	6.7
	9	10	3	1.2	7.2	1.8	6.5	1.4	8.1	1.3	5.5
Acceleration + Displacement	10	4	NO	2.0	13.1	3.2	10.4	2.6	15.1	2.4	8.4
	11	4	2	2.2	14.0	3.9	12.3	3.6	10.8	2.3	18.1
	12	4	3	2.1	12.9	3.4	11.1	3.5	11.4	2.1	16.9
	13	6	NO	1.4	3.1	3.0	9.9	1.8	1.4	2.0	10.3
	14	6	2	2.6	22.3	4.6	13.8	4.8	17.5	2.7	21.5
	15	6	3	1.9	6.0	3.6	12.0	2.6	3.6	2.3	15.8
	16	10	NO	2.8	22.4	3.2	10.0	4.0	24.8	2.7	6.1
	17	10	2	1.7	6.0	3.2	10.9	2.0	7.1	2.2	11.6
	18	10	3	1.8	4.3	3.3	11.5	2.1	5.1	2.2	13.8

obtained, which indicated good prediction capabilities for unobserved responses using the proposed approach. Displacement-related responses (curvature and strain) exhibited larger errors than force-related responses (moment and stress), which is consistent with results obtained for measured responses. These trends are attributed to displacement-related responses being more sensitive to low-frequency drift from the estimated input. Note that RRMSEs larger than 15% are shaded in grey in Table 4. Fig. 11 compares true and predicted unmeasured responses for case studies ID1 and ID18 and similar agreement is obtained. The roof drift ratio (RDR) and base shear in the transverse direction normalized
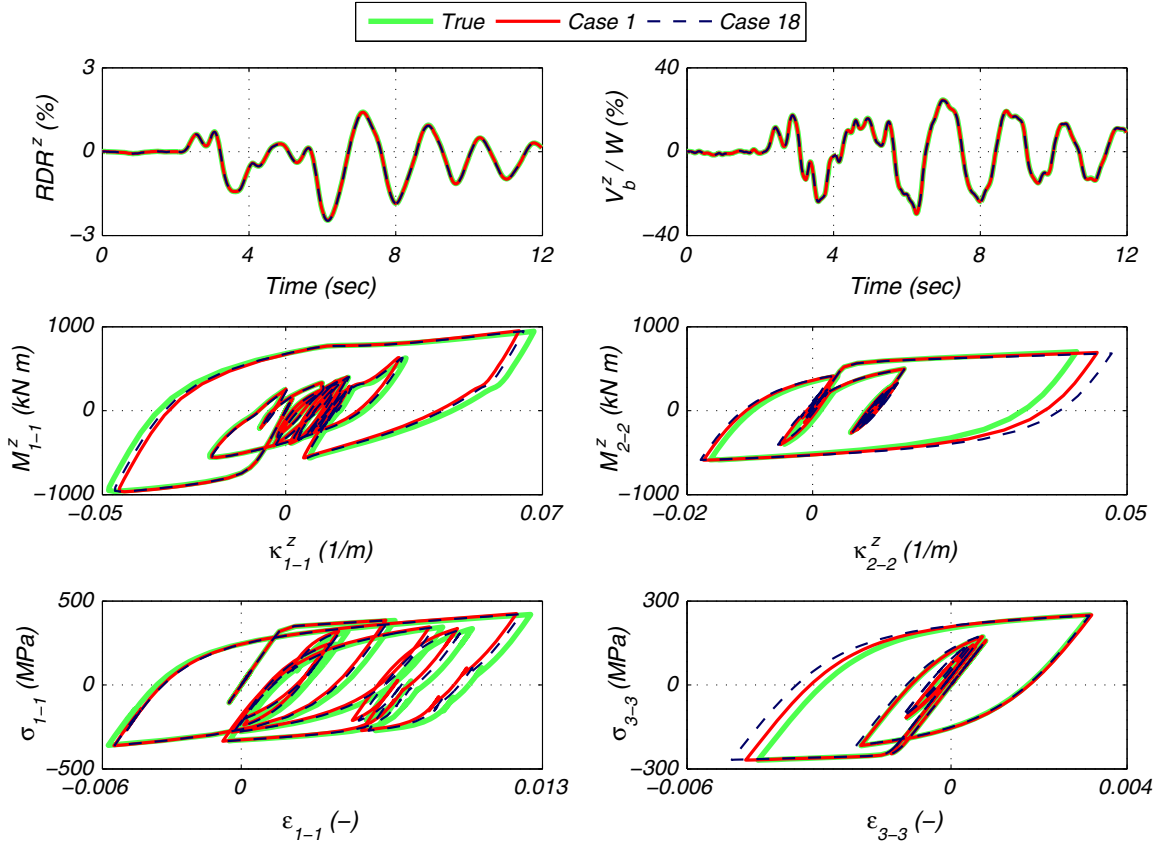
Fig. 11. Comparison between true and estimated unmeasured responses for Cases ID1 and ID18.

by the total weight of the building (V_b/W), both global response measures, are shown and also demonstrate excellent agreement.

4.7. Parametric studies on the filter parameters

It is well-known that the performance of Kalman-based filters is influenced by the four variables defining them, i.e. initial estimate ($\hat{\theta}_{0|0}$), initial covariance ($\hat{\mathbf{P}}_{0|0}^{\theta\theta}$), process noise covariance ($\mathbf{Q}$), and measurement noise covariance ($\mathbf{R}$). To analyze the effects of these variables in the estimation results of the framework proposed in this paper, a set of nine parametric studies was conducted. As a reference, case ID1 was considered, i.e., acceleration-only response, $p = 4$, and no-iterations. The estimation results for the parametric studies are summarized in Table 5. Note that in this table $\hat{\theta}_{0|0}^{fem,1} = \begin{bmatrix} 1.4 \cdot E_{col}^{true} & 0.7 \cdot f_{col}^{true} & 0.8 \cdot b_{col}^{true} & 1.5 \cdot E_{beam}^{true} & 0.8 \cdot f_{beam}^{true} & 1.3 \cdot b_{beam}^{true} \end{bmatrix}^T$, $\hat{\theta}_{0|0}^{fem,2} = \begin{bmatrix} 0.5 \cdot E_{col}^{true} & 2.0 \cdot f_{col}^{true} & 1.4 \cdot b_{col}^{true} \\ 0.6 \cdot E_{beam}^{true} & 1.5 \cdot f_{beam}^{true} & 1.3 \cdot b_{beam}^{true} \end{bmatrix}^T$, and the coefficients shown for $\hat{\mathbf{P}}_{0|0}^{\theta\theta}$ and $\mathbf{Q}$ represents the factor r in the (i,i) entry of the diagonal matrices $\left(\hat{\mathbf{P}}_{0|0}^{\theta\theta} \right)_{i,i} = \left(r \times \hat{\theta}_{0|0} \right)_i^2$ and $\mathbf{Q}_{i,i} = \left(r \times \hat{\theta}_{0|0} \right)_i^2$, respectively. As observed from the table, very good estimation results were obtained for different values of the parameters defining the filter, except when the initial covariance of the TAR model parameters is low (case PS3) and when the initial estimate of the parameters is far from the true values and the initial covariance of the FE model parameters is low ($r = 0.05$) (case PS7). In the former case, considering 2 iterations allowed to improve the estimation and achieve excellent results. In the latter, considering 2 iterations ($N_{iter} = 2$) or increasing the initial covariance of the FE model parameters implied that the filter accurately estimates the input and appropriately update the FE model. These parametric studies clearly show that the proposed framework is robust and that appropriate definition of the variables involved in the algorithm provides accurate estimation results. Note that in Table 5, cells shaded in green refer to the filter parameters modified with respect to case ID1, while cells shaded in red indicate cases for which no proper estimation is achieved.

Table 5
Results of parametric studies on the filter parameters (all with acceleration-only response and $p = 4$).

Case	$\hat{\theta}_{0\|0}^{fem}$	$\hat{P}_{0\|0}^{00}$		Q		R	N_{iter}	Normalized model parameter estimate						$RRMSE_{input}$ (%)
		FE model	TAR model	FE model	TAR model	$(m/s^2)^2$		$\dfrac{E_{col}}{E_{col}^{true}}$	$\dfrac{f_{col}}{f_{col}^{true}}$	$\dfrac{b_{col}}{b_{col}^{true}}$	$\dfrac{E_{beam}}{E_{beam}^{true}}$	$\dfrac{f_{beam}}{f_{beam}^{true}}$	$\dfrac{b_{beam}}{b_{beam}^{true}}$	
PS1	$\hat{\theta}_{0\|0}^{fem,1}$	0.05	1.00	1e-5	1e-5	9×10^{-4}	NO	1.00	1.00	1.10	1.00	1.01	0.81	11.9
PS2	$\hat{\theta}_{0\|0}^{fem,1}$	0.05	1.00	1e-6	1e-6	9×10^{-4}	NO	1.00	1.00	1.10	1.00	1.01	0.80	12.2
PS3	$\hat{\theta}_{0\|0}^{fem,1}$	0.05	0.10	1e-6	1e-5	9×10^{-4}	NO	0.93	0.88	1.53	1.06	0.88	3.96	100.0
PS4	$\hat{\theta}_{0\|0}^{fem,1}$	0.05	0.10	1e-6	1e-5	9×10^{-4}	2	1.00	1.00	1.10	1.00	1.01	1.00	6.8
PS5	$\hat{\theta}_{0\|0}^{fem,1}$	0.15	0.10	1e-6	1e-5	9×10^{-4}	NO	1.00	1.01	1.03	1.00	1.01	0.78	10.5
PS6	$\hat{\theta}_{0\|0}^{fem,1}$	0.05	1.00	1e-6	1e-5	2×10^{-5}	NO	1.00	1.02	1.32	0.99	0.98	1.26	13.8
PS7	$\hat{\theta}_{0\|0}^{fem,2}$	0.05	1.00	1e-6	1e-5	9×10^{-4}	NO	0.93	0.88	1.67	1.05	0.87	4.52	100
PS8	$\hat{\theta}_{0\|0}^{fem,2}$	0.05	1.00	1e-6	1e-5	9×10^{-4}	2	1.00	1.00	1.02	1.00	1.00	0.90	12.3
PS9	$\hat{\theta}_{0\|0}^{fem,2}$	0.15	1.00	1e-6	1e-5	9×10^{-4}	2	1.00	1.00	1.02	1.00	1.00	0.86	12.2

Table 6
Wall-clock time to complete the estimation process.

Response measurement	Case ID	p	N_{iter}	Wall-clock time (h)
Acceleration	1	4	NO	2.7
	2	4	2	5.2
	3	4	3	7.7
	4	6	NO	4.0
	5	6	2	7.2
	6	6	3	9.1
	7	10	NO	4.8
	8	10	2	9.4
	9	10	3	14.5
Acceleration + Displacement	10	4	NO	2.5
	11	4	2	5.1
	12	4	3	8.0
	13	6	NO	3.7
	14	6	2	7.1
	15	6	3	8.8
	16	10	NO	5.1
	17	10	2	9.7
	18	10	3	15.4

From all the analyses conducted, it is suggested to consider a low to moderate initial covariance of the FE model parameters ($r = 0.05$ to $r = 0.15$), a high initial covariance of the TAR model parameters ($r = 1.00$), and low values for the diagonal terms in the process noise covariance matrix $\mathbf{Q}$ ($r = 1e-5$ or $r = 1e-6$). Based on the results obtained, the approach is robust to the measurement noise covariance $\mathbf{R}$.

4.8. Computational cost

An algorithm computational cost plays an important role when selecting a framework, since quickly knowing structural conditions and possible damage is of vital importance when making decisions after an extreme event. Table 6 lists wall-clock time required for the estimation process for each case study. Note that all results were obtained from analyses performed using 8 cores from a desktop workstation having an Intel Xeon E5-2650 (2.3 GHz) processor and 64 GB random-access mem-

ory. As pointed out by other researchers, UKF can take advantage of parallel processor capabilities and using more cores can efficiently decrease computation times [54,55].

As anticipated, computational cost increases significantly as iterations and higher TAR model orders are considered. However, based on presented results a low TAR model order and no iterations achieves very good estimation results, almost identical to those obtained using higher order TAR models with iterations. It is concluded that $p = 4$ without iterations is a good combination to properly estimate unknown FE model parameters and input excitations.

5. Conclusions

This study proposed a new framework for calibration of nonlinear structural finite element (FE) models subjected to unknown excitations using response time histories obtained from a sparse sensor network. It was initially shown that seismic excitation sources could be effectively reconstructed using relatively low order time-varying auto-regressive (TAR) models. A novel iterative Kalman filter (KF) was developed to recursively estimate TAR model parameters when past seismic excitation source measurements were available. The framework was further extended to cases with unknown parameters of the structural model and no seismic excitation measurements being available. For these cases TAR model parameters are estimated solely based on measured structural response. The proposed output-only nonlinear FE model updating framework employs an unscented Kalman filter (UKF) to jointly estimate FE and TAR model parameters using sparsely measured global structural response quantities. Extensive numerical analyses were conducted on a realistic three-dimensional steel frame, assuming unknown material model parameters and seismic excitations, to validate the applicability of the proposed framework. TAR models with various orders were considered and, additionally, analyses featuring various numbers of iterations were compared. It was concluded that the proposed framework allows for proper calibration of nonlinear FE models and proper reconstruction of seismic excitations using estimated TAR model parameters. TAR model orders as low as 4 involving no filtering iterations step provide precise input identification and unbiased FE model parameter estimates, thus providing a computationally efficient algorithm for parameter-input estimation of nonlinear structural models. It was observed that the estimation did not improve when heterogeneous responses (i.e. absolute acceleration and relative displacement) were considered. In addition, it was shown that global and local responses predicted using the calibrated FE model and estimated input excitation are in very good agreement with true responses for both measured and unmeasured response quantities. Acceleration and force-related responses (moment and stress) were better predicted than strain, curvature, and displacement responses, with low frequency drift in the estimated input most likely causing the increased error for the displacement-related responses. Although the case study presented includes one unknown input component and six unknown model parameters, the mathematical formulation proposed is general and it does not limit the number of model parameter or number of unknown input components.

CRediT authorship contribution statement

J. Castiglione: Software, Investigation, Writing - original draft. **R. Astroza:** Conceptualization, Methodology, Supervision, Writing - original draft, Writing - review & editing. **S. Eftekhar Azam:** Methodology, Writing - original draft. **D. Linzell:** Writing - review & editing.

Declaration of Competing Interest

The authors declare that they have no known competing financial interests or personal relationships that could have appeared to influence the work reported in this paper.

Acknowledgements

Appendix A. Supplementary data

Supplementary data to this article can be found online at https://doi.org/10.1016/j.ymssp.2020.106779.

References

[1] N. Distefano, A. Rath, Sequential identification of hysteretic and viscous models in structural seismic dynamics, Comput. Methods Appl. Mech. Eng. 6 (1975) 219–232.
[2] E.P. Carden, P. Fanning, Vibration based condition monitoring: a review, Struct. Health Monit. 3 (2004) 355–377.
[3] R.E. Kalman, A new approach to linear filtering and prediction problems, J. Basic Eng. 82 (1960) 35–45.

[4] P.K. Kitanidis, Unbiased minimum-variance linear state estimation, Automatica 23 (1987) 775–778.
[5] C.S. Hsieh, Robust two-stage Kalman filters for systems with unknown inputs, IEEE Trans. Autom. Control 45 (2000) 2374–2378.
[6] S. Gillijns, B. De Moor, Unbiased minimum-variance input and state estimation for linear discrete-time systems, Automatica 43 (2007) 111–116.
[7] S. Gillijns, B. De Moor, Unbiased minimum-variance input and state estimation for linear discrete-time systems with direct feedthrough, Automatica 43 (2007) 934–937.
[8] E. Lourens, C. Papadimitriou, S. Gillijns, E. Reynders, G. De Roeck, G. Lombaert, Joint input-response estimation for structural systems based on reduced-order models and vibration data from a limited number of sensors, Mech. Syst. Sig. Process. 29 (2012) 310–327.
[9] O. Sedehi, C. Papadimitriou, D. Teymouri, L.S. Katafygiotis, Sequential Bayesian estimation of state and input in dynamical systems using output-only measurements, Mech. Syst. Signal Process. 131 (2019) 659–688.
[10] S. Eftekhar Azam, E. Chatzi, C. Papadimitriou, A dual Kalman filter approach for state estimation via output-only acceleration measurements, Mech. Syst. Sig. Process. 60 (2015) 866–886.
[11] E. Lourens, E. Reynders, G. De Roeck, G. Degrande, G. Lombaert, An augmented Kalman filter for force identification in structural dynamics, Mech. Syst. Sig. Process. 27 (2012) 446–460.
[12] S. Eftekhar Azam, E. Chatzi, C. Papadimitriou, A. Smyth, Experimental validation of the Kalman-type filters for online and real-time state and input estimation, J. Vib. Control 23 (2017) 2494–2519.
[13] Ø.W. Petersen, O. Øiseth, T.S. Nord, E. Lourens, Estimation of the full-field dynamic response of a floating bridge using Kalman-type filtering algorithms, Mech. Syst. Signal Process. 107 (2018) 12–28.
[14] K. Maes, K.V. Nimmen, E. Lourens, A. Rezayat, P. Guillaume, G.D. Roeck, et al, Verification of joint input-state estimation for force identification by means of in situ measurements on a footbridge, Mech. Syst. Sig. Process. 75 (2016) 245–260.
[15] M. Hoshiya, E. Saito, Structural identification by extended Kalman filter, J. Eng. Mech. 110 (1984) 1757–1770.
[16] S.J. Julier, J.K. Uhlmann, H.F. Durrant-Whyte, A new approach for filtering nonlinear systems, American Control Conference, 1995, Seattle, Washington, USA.
[17] S. Eftekhar Azam, S. Mariani, Dual estimation of partially observed nonlinear structural systems: a particle filter approach, Mech. Res. Commun. 46 (2012) 54–61.
[18] W. Song, Generalized minimum variance unbiased joint input-state estimation and its unscented scheme for dynamic systems with direct feedthrough, Mech. Syst. Sig. Process. 99 (2018) 886–920.
[19] Z. Wan, T. Wang, S. Li, Z. Zhang, A modified particle filter for parameter identification with unknown inputs, Struct. Control Health Monit. 25 (2018) e2268.
[20] Y. Lei, Y. Jiang, Z. Xu, Structural damage detection with limited input and output measurement signals, Mech. Syst. Sig. Process. 28 (2012) 229–243.
[21] R. Tipireddy, H. Nasrellah, C. Manohar, A Kalman filter based strategy for linear structural system identification based on multiple static and dynamic test data, Prob. Eng. Mech. 24 (2009) 60–74.
[22] E.N. Chatzi, A.W. Smyth, Particle filter scheme with mutation for the estimation of time-invariant parameters in structural health monitoring applications, Struct. Control Health Monit. 20 (2013) 1081–1095.
[23] C.-K. Ma, C.-C. Ho, An inverse method for the estimation of input forces acting on non-linear structural systems, J. Sound Vib. 275 (2004) 953–971.
[24] S.M. Bittanti, A. Nappi, Inverse problems in structural elastoplasticity: a Kalman filter approach, in: A. Sawczuk, G. Bianchi, (Eds.), Plasticity Today, Elsevier Applied Science Publishers, 1984, pp. 311–329.
[25] G. Bolzon, R. Fedele, G. Maier, Parameter identification of a cohesive crack model by Kalman filter, Comput. Methods Appl. Mech. Eng. 191 (2002) 2847–2871.
[26] R. Astroza, H. Ebrahimian, J. Conte, Material parameter identification in distributed plasticity FE models of frame-type structures using nonlinear stochastic filtering, J. Eng. Mech. (2014) 04014149.
[27] H. Ebrahimian, R. Astroza, J.P. Conte, Extended Kalman filter for material parameter estimation in nonlinear structural finite element models using direct differentiation method, Earthq. Eng. Struct. Dyn. (2015).
[28] J.N. Yang, S. Pan, H. Huang, An adaptive extended Kalman filter for structural damage identifications II: unknown inputs, Struct. Control Health Monit. 14 (2007) 497–521.
[29] Y. Lei, C. Liu, L. Liu, Identification of multistory shear buildings under unknown earthquake excitation using partial output measurements: numerical and experimental studies, Struct. Control Health Monit. 21 (2014) 774–783.
[30] F. Naets, J. Croes, W. Desmet, An online coupled state/input/parameter estimation approach for structural dynamics, Comput. Methods Appl. Mech. Eng. 283 (2015) 1167–1188.
[31] K. Maes, F. Karlsson, G. Lombaert, Tracking of inputs, states and parameters of linear structural dynamic systems, Mech. Syst. Sig. Process. 130 (2019) 755–775.
[32] Z. Wan, T. Wang, L. Li, Z. Xu, A novel coupled state/input/parameter identification method for linear structural systems, Shock Vib. 2018 (2018).
[33] S. Pan, D. Xiao, S. Xing, S. Law, P. Du, Y. Li, A general extended Kalman filter for simultaneous estimation of system and unknown inputs, Eng. Struct. 109 (2016) 85–98.
[34] V.K. Dertimanis, E. Chatzi, S.E. Azam, C. Papadimitriou, Input-state-parameter estimation of structural systems from limited output information, Mech. Syst. Sig. Process. 126 (2019) 711–746.
[35] Y. Lei, D. Xia, K. Erazo, S. Nagarajaiah, A novel unscented Kalman filter for recursive state-input-system identification of nonlinear systems, Mech. Syst. Sig. Process. 127 (2019) 120–135.
[36] S. Sen, A. Crinière, L. Mevel, F. Cérou, J. Dumoulin, Seismic-induced damage detection through parallel force and parameter estimation using an improved interacting Particle-Kalman filter, Mech. Syst. Sig. Process. 110 (2018) 231–247.
[37] H. Ebrahimian, R. Astroza, J.P. Conte, C. Papadimitriou, Bayesian optimal estimation for output-only nonlinear system and damage identification of civil structures, Struct. Control Health Monit. 25 (2018) e2128.
[38] K. Erazo, S. Nagarajaiah, An offline approach for output-only Bayesian identification of stochastic nonlinear systems using unscented Kalman filtering, J. Sound Vib. 397 (2017) 222–240.
[39] R. Astroza, H. Ebrahimian, Y. Li, J.P. Conte, Bayesian nonlinear structural FE model and seismic input identification for damage assessment of civil structures, Mech. Syst. Sig. Process. 93 (2017) 661–687.
[40] M.K. Chang, J.W. Kwiatkowski, R.F. Nau, R.M. Oliver, K.S. Pister, ARMA models for earthquake ground motions, Earthq. Eng. Struct. Dyn. 10 (1982) 651–662.
[41] M. Spiridonakos, S. Fassois, Non-stationary random vibration modelling and analysis via functional series time-dependent ARMA (FS-TARMA) models – a critical survey, Mech. Syst. Sig. Process. 47 (2014) 175–224.
[42] S. Rezaeian, A. Der Kiureghian, Simulation of synthetic ground motions for specified earthquake and site characteristics, Earthq. Eng. Struct. Dyn. 39 (10) (2010) 1155–1180.
[43] J.P. Conte, B.F. Peng, Fully nonstationary analytical earthquake ground-motion model, J. Eng. Mech. 123 (1) (1997) 15–24.
[44] M. Spiridonakos, E.N. Chatzi, Metamodeling of dynamic nonlinear structural systems through polynomial chaos NARX models, Comput. Struct. 157 (2015) 99–113.
[45] M. Spiridonakos, E.N. Chatzi, Metamodeling of nonlinear structural systems with parametric uncertainty subject to stochastic dynamic excitation, Earthq. Struct. 8 (4) (2015) 915–934.
[46] R. Astroza, N. Barrientos, Y. Li, E. Saavedra Flores, Z. Liu, Bayesian updating of complex nonlinear FE models with high-dimensional parameter space using heterogeneous measurements and a batch-recursive approach, Eng. Struct. 201 (109724) (2019) 1–21.
[47] ICC, International Building Code, in: Falls Church, VA, ed: International Code Council, 2012.

[48] S. Mazzoni, F. McKenna, G.L. Fenves, Opensees Command Language Manual, Pacific Earthquake Engineering Research, Berkeley, California, USA, 2005.
[49] F.F. Taucer, E. Spacone, F.C. Filippou, A Fiber Beam-Column Element for Seismic Response Analysis of Reinforced Concrete Structures, Earthquake Engineering Research Center, University of California, Berkeley, 1991.
[50] F.C. Filippou, E.P. Popov, V.V. Bertero, Bond Deterioration on Hysteretic Behavior of Reinforced Concrete Joints, Earthquake Engineering Research Center, University of California, Berkeley, 1983.
[51] H. Ebrahimian, R. Astroza, J.P. Conte, R.R. Bitmead, Information-theoretic approach for identifiability assessment of nonlinear structural finite-element models, J. Eng. Mech. 145 (2019) 04019039.
[52] K.A. Porter, J.L. Beck, R.V. Shaikhutdinov, Sensitivity of building loss estimates to major uncertain variables, Earthq. Spectra 8 (2002) 719–743.
[53] K. Maes, M. Chatzis, G. Lombaert, Observability of nonlinear systems with unmeasured inputs, Mech. Syst. Sig. Process. 130 (2019) 378–394.
[54] R. Astroza, H. Ebrahimian, J. Conte, Performance comparison of Kalman−based filters for nonlinear structural finite element model updating, J. Sound Vib. 438 (2019) 520–542.
[55] S. Eftekhar Azam, A. Ghisi, S. Mariani, Parallelized sigma-point Kalman filtering for structural dynamics, Comput. Struct. 92–93 (2012) 193–205.